Available online at www.sciencedirect.com
ScienceDirect
ELSEVIER
Nuclear Physics B (Proc. Suppl.) 165 (2007) 11–18
NUCLEAR PHYSICS B PROCEEDINGS SUPPLEMENTS
www.elsevierphysics.com

Recent Results from the High Resolution Fly's Eye Experiment: An Introduction

P. Sokolsky[a] presented on behalf of the High Resolution Fly's Eye Collaboration

[a]High Energy Astrophysics Institute
University of Utah
Salt Lake City, Utah, USA 84112

The HiRes experiment has now completed data taking. We describe the experiment, the detector and atmospheric calibration and studies to improve precision of knowledge of air-fluorescence efficiency. The current results on the monocular and stereo spectrum and stereo-based composition measurements are summarized. Possible correlation of stereo data event directions with a subset of Bl-Lac objects is discussed.

1. Introduction

This paper describes the High Resolution Fly's Eye (HiRes) experiment and introduces physics results on the spectrum, compostion and anisotropy of ultra-high energy cosmic rays. More detailed descriptions of these results can be found in other papers presented at this conference.

The HiRes experiment consists of two sites (HiRes I and II) 12.6 km apart, located at Dugway proving Ground in Utah. Each site consists of telescope units (22 at HiRes I and 42 at HiRes II) pointing at different parts of the sky. The detectors observe the full 360 degrees in azimuth but cover from 3 to 16.5 (Hires I) and from 3 to 30 degrees (HiRes II) in elevation angles. Since most cosmic ray events in this energy range are detected at distances of between 5 and 30 km from the detectors, higher elevation angles contribute little to the event rate. Each telescope consists of a 3.72 m^2 effective area mirror and a 256 phototube camera cluster in the mirror focal plane. The phototubes subtend a one degree by one degree field of view on the sky. The tubes view signals through a UV filter which cuts out light below 300 nm and above 400 nm (corresponding to the air-fluorescence spectral range).

2. Event Reconstruction

The arrival direction of the cosmic ray initiating the shower can be reconstructed monocularly, using the triggered tube pointing directions to determine the shower-detector plane, and the relative tube triggering times to determine the impact parameter and angle of the track within the plane. From this information, the impact parameter, zenith and azimuth angles can be easity calculated. Stereo reconstruction affords much better precision. If the shower is detected by both HiRes I and II and two shower-detector planes are determined for the event, the shower direction must lie along the intersection of the two planes. Because of the simplicity of the method, it is virtually impossible to get the shower direction and distance systematically wrong, once the pointing directions for the phototubes are accurately determined.

The largest data sample consists of events seen by HiRes I only, since this detector turned on three years before the completion of Hires II. Because of the limited elevation angle coverage of HiRes I monocular events are too short in angular spread for reliable determination of the geometry by timing alone. Experiment and simulation have shown that while the position of an EAS in the atmosphere will fluctuate, its shape has very little variation. This shape is well described by the Gaisser-Hillas function. To improve resolution for the HiRes I data, the expected form of the shower development (i.e. the shape of its longitudinal profile) is used to constrain the time fit. The HiRes II event sample has longer track lengths and the geometry can be well determined from timing alone. The profile constrained HiRes I fit has been carefully checked using both simulations and comparisons of reconstruction with stereo data for the subset of events where HiRes II was also triggered.

Once the geometry of the event is determined, the tube signals are used to determine the shower size in one degree angular bins on the sky (for HiRes I), or in time bins corresponding to the FADC clock at HiRes II. Finally, combining the bin signal, corrected for atmospheric attenuation, with knowledge of the shower geometry, we calculate the size of

0920-5632/$ – see front matter
doi:10.1016/j.nuclphysbps.2006.11.003

the shower as a function of atmospheric depth. Cherenkov light scattered into the detector is subtracted in an iterative process. The depth of shower maximum, Xmax, and shower energy E are determined from the Gaisser-Hillas fit to the profile. The shower energy is proportional to the integral of the Gaisser-Hillas function after corrections are made for missing energy due to neutral particles or high-energy muons hitting the earth's surface. The missing energy correction (~10%)is weakly hadronic model dependent.

An example of a longitudinal shower profile of a stereo event is shown in Fig. 1.

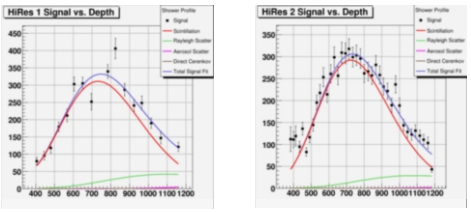

Fig. 1 Typical shower profile measured by HiRes I and HiRes II

3. Detector Calibration

The energy scale of air-fluorescence detectors depends on a number of factors including the air-fluorescence efficiency, the effect of scattering in the atmosphere, the gain and efficiency of the phototubes and the reflectivity of the mirrors. The absolute calibration of the phototubes is done with a portable Xenon light source whose stability is better than 2% [1]. The source is mounted in the center of the mirror and illuminates the pmt cluster uniformly. The source is moved from mirror to mirror and its intensity is separately calibrated using photoelectron statistics, NIST-traceable photodiodes and HPD tubes. The night to night relative gain of the phototubes is monitored using a YAG laser whose output is sent out to all the mirrors via quartz optical fibers. In addition a portable laser positioned at 4 km from each mirror is used to cross-check the end to end detetector calibration. Mirror reflectivity is measured separately using a commercial UV reflectometer. The tube and mirror calibration constants are known to a 10% accuracy.

4. Atmospheric measurements and calibration

There are three components of the atmosphere that are of importance to air-fluorescence measurements: the molecular atmospheric density profile, the aerosol component and the presence and distribution of clouds in the detector aperture [2]. The molecular component is stable, exhibiting small seasonal dependence. We use radiosonde balloon data from the Salt Lake City airport (~ 100 km away) to correct for daily and seasonal density variation (see Fig.2).

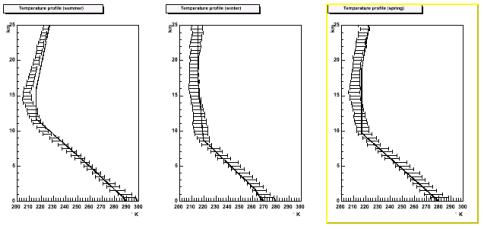

Fig. 2 Molecular density profiles measured from radiosond data at Salt Lake airport versus seasonal model predictions.

Aerosols can vary in horizontal and vertical profile on short time scales. We monitor the aerosols by firing steerable UV lasers from both HiRes I and HiRes II detector sites. The other detector triggers on light scattered out of the laser beam by a combination of molecular (Rayleigh) and aerosol scattering. Since the molecular component is well know we subtract out this contribution and we determine the VAOD, the vertical aerosol optical depth, on an hourly basis [2]. The various laser measurements allow us to reconstruct the horizontal scattering length and the exponential scale height of the aerosols. Fig. 3 shows a typical distribution of VAOD over a year, indicating that the attenuation from this source is small when compared to the known molecular scattering.

Clouds can be detected by a number of techniques, including visual observation, IR temperature measurements of the night sky seen by the mirrors, and the characteristic enhancement of light scattering out of a laser beam as it sweeps through a cloud.

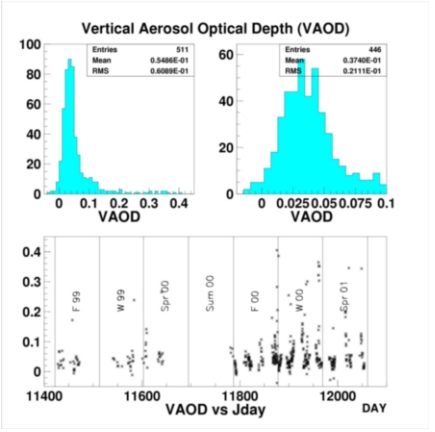

Fig. 3 Vertical Aerosol Optical Depth (VAOD) over a year's period.

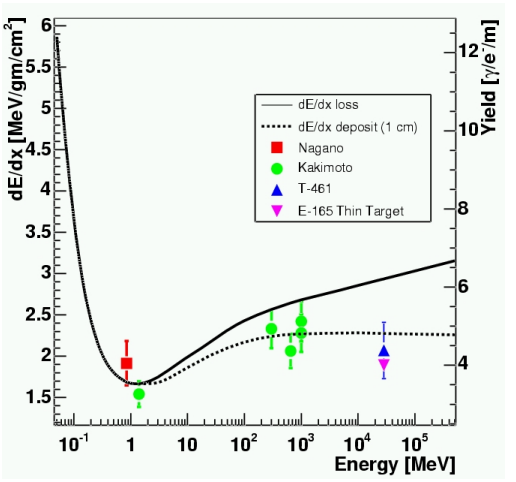

Fig. 4 The air-fluorescence efficiency integrated over the HiRes wavelength window as a function of electron energy.

Phototube gain and efficiency, mirror reflectivity, atmospheric attenuation and the presence of clouds are stored in an extensive data base on an hourly basis. This database is used both in reconstructing real events and in generating simulated Monte Carlo data.

5. Air Fluorescence Efficiency

A number of experiments have measured the air-fluorescence efficiency, using radioactive sources or electron beams [3]. Most recently, a subset of the Hires collaboration (the E-165 collaboration) has performed an experiment at SLAC to determine the air-fluroescence efficency more precisely [4]. The current data is shown in Fig 4 and is in good agreement with the energy deposited in the gas via the dE/dX curve.

The shape of the shower profile as determined by air fluorescence was also measured by this group in a follow-up thick target experiment [5]. Fig. 5 shows the comparison of the fluorescence signal as a function of radiation length into a shower with a fit to GEANT predictions for 28.5 GeV electrons. In this case, the SLAC electron beam interacted in an Alumina air equivalent target.

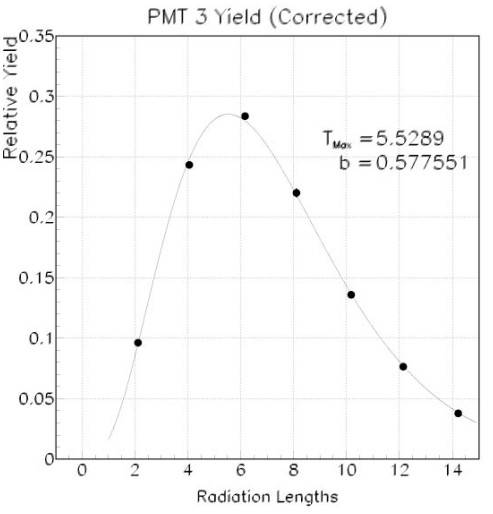

Fig. 5. Comparison of fit to GEANT prediction (curve) with measured air fluorescence yield (solid points). (Statistical) error bars are smaller than data points.

6. Cosmic Ray Spectrum

Because of the different turn-on times of HiRes I and HiRes II and the different elevation angle coverage of the two detectors, we have three different data sets in the analysis: HiRes I monocular, HiRes II monocular, and HiRes stereo data. HiRes I monocular has the largest statistics and utilizes the profile constrained monocular timing reconstruction technique [6]. This has an effective physics threshold of near 3 EeV, determined by rapidly worsening energy resolution below this threshold. HiRes II, in contrast, has a physics energy threshold of near .2 EeV, set by rapidly changing aperture below this energy. The stereo data has an effective energy threshold of 2 EeV, again set by the onset of a rapidly decreasing aperture below this energy. The monocular aperture grows with energy and must be carefully simulated [7]. The most recent monocular spectrum from HiRes I and II is shown in Fig 6. The spectrum clearly exhibits an ankle with a spectral minimum near 3-5 EeV and a depletion of events above 80 EeV consistent with the GZK feature [8]. Details of the analysis and the physical interpretation of the ankle and GZK suppression features can be found in the paper by D. Bergman in this proceeding s.

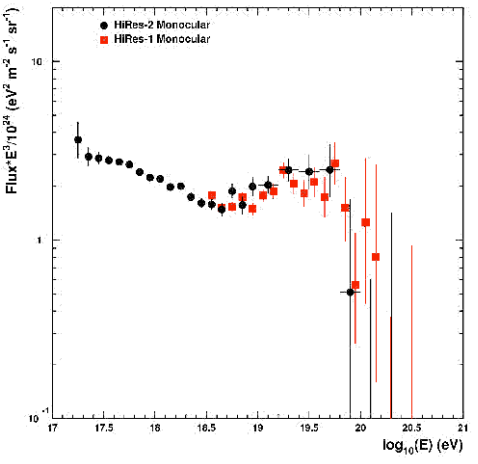

Fig. 6 Most recent monocular spectrum. Black points are HiRes II data. Red points are HiRes I data.

From the point of view of geometrical reconstruction, the most reliable spectral data comes from the stereo data set. However, since the stereo aperture is the intersection of two monocular apertures, the aperture calculation is more complex and the aperture drops very rapidly below 2 EeV. Fig. 7 shows the stereo spectrum superimposed on the monocular spectra. There is excellent agreement between the two.

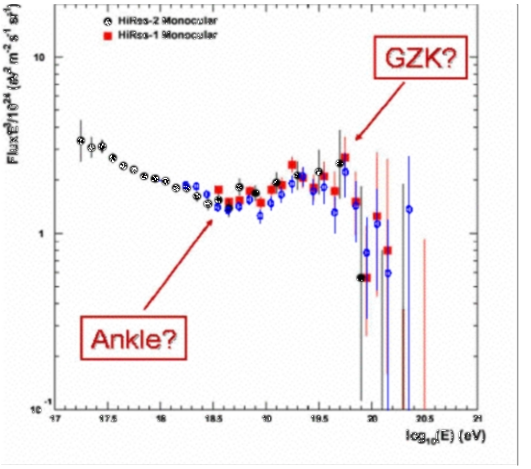

Fig. 7 Stereo spectrum (blue diamonds) superimposed on monocular spectrum. Note monocular spectrum in this figure corresponds to a smaller data set than in Fig. 6

One of the advantages of stereo reconstruction is that the same shower is measured by two different detectors. This allows us to check the energy resolution of the sytem, without relying so much on simulations. Fig. 8 shows the distribution of energies of showers where the energy had a separate determination in HiRes I and HiRes II. The distribution is Gaussian and its width is consistent with expectations from simulation. The inferred HiRes II energy resolution is ~15%.

Since the stereo spectrum exhibits significant structure (the ankle and the GZK cutoff), it is important to establish that this structure is not the result of systematics in the determination of the stereo aperture. To study this, we define a "fully efficient" stereo aperture, where both HiRes I and HiRes II detectors will trigger with maximal efficiency.

This is done by defining, for each energy bin, a maximum Rp from each detector, such that for showers with smaller impact parameters will always trigger both detectors. This is illustrated by the curve in Fig. 9. Data points below the the curve fall into the "fully efficient" region of the aperture. Fig. 10 shows the resultant stereo spectrum. It is consistent with the ordinary stereo aperture and exhibits the same features.

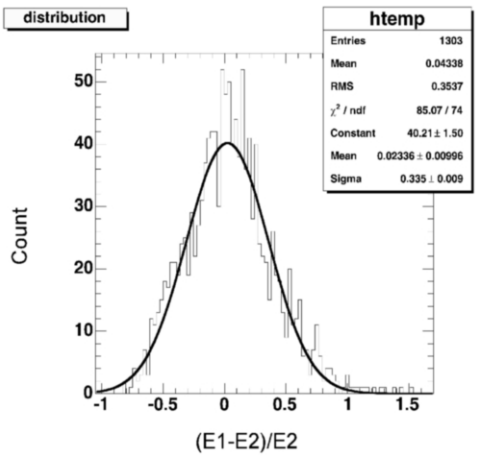

Fig. 8 Distribution of energy differences between HiRes I and HiRes II. Width is consistent with expected energy resolution

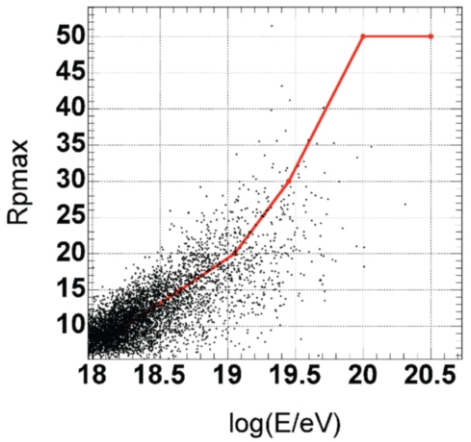

Fig. 9 Rp vs energy for stereo events. Solid curve shows region of "full efficiency"

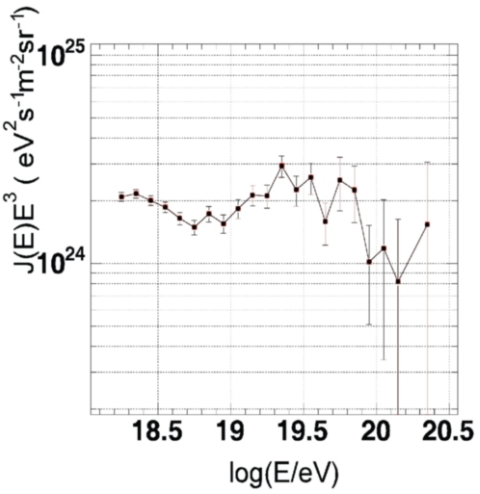

Fig. 10 "Fully efficient" stereo spectrum.

The observed features are independent of the way we define the stereo aperture. Note that both stereo spectrum figures do not have final cloud free aperture cuts and hence are preliminary.

7. Cosmic Ray Composition

The distribution of shower maxima (Xmax) is known to be sensitive to the composition of cosmic rays. Both the elongation rate and the absolute position of the mean Xmax and its fluctuations about the mean carry information about the primary composition [9]. While the detailed interpretation is hadronic model dependent, a measure of the systematic uncertainties can be garnered by comparing the predictions of a variety of hadronic models, from QGS-Jet and Sybbil to DPM jet [10]. The elongation rate, or slope of the mean Xmax per decade of energy, is essentially model independent up to energies of 30 to 50 EeV and the variation in absolute mean Xmax position are in agreement to within 25-30 gm/cm^2 in this energy region. Since the separation between a pure Fe and a pure p spectrum is about 70-100 gm/cm^2, qualitative information about the nature of the primary particles can certainly be had using this technique.

Fig. 11 shows the elongation rate from the stereo data [11]. Also included in this figure are lower energy data from an earlier hybrid experiment [12]. Above 1 EeV, the data is consistent with a light, mainly protonic composition. However, this HiRes data is based on the first two years of operation and runs out of statistics above 30 EeV. We have recently analyzed a much larger sample of stereo events, with stringent shower profile quality cuts. These "golden events" yield an extension to the elongation rate to nearly 100 EeV (see Fig. 12). HiRes Xmax data is consistent with a light composition to the highest energies.

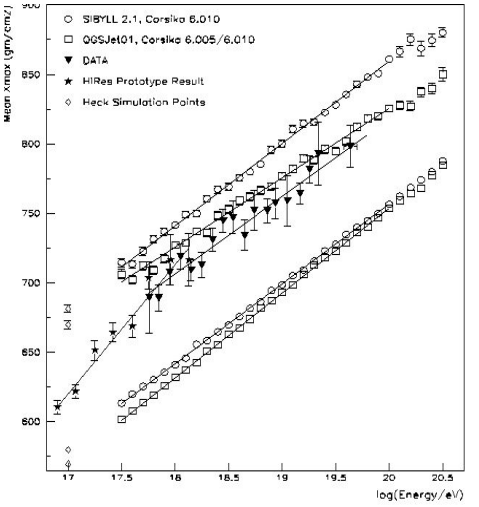

Fig. 11 HiRes stereo data elongation rate. Also shown is the result from the HiRes prototype/MIA experiment

9. Anisotropy

A detailed report on studies of the anisotropy of ultra-high energy cosmic rays using the HiRes monocular and stereo data set can be found in the contribution to these proceedings by John Belz. No significant large-scale anisotropies have been found in the data [13]. Here we mention an intriguing small scale anisotropy in the stereo data, which was first pointed out by Gorbunov et al. 14].

Tyniakov et al. have suggested that well identified Bl-Lac objects are attractive candidates for cosmic ray acceleration [15]. Initial binned analysis of HiRes stereo data directions relative to the Veron catalogue of Bl-Lacs with a magnitude < 18 cut yielded a marginally significant correlation within the angular resolution of the HiRes detector. We have done a detailed maximum likelihood analysis of this correlation and have broadened the target catalogue to include HP (high polarization) Bl-Lacs as well [16]. With no energy cut, we find evidence for ~22 such objects being correlated with observed cosmic ray directions within the .6 degree Hires stereo resolution with an estimated probability of 10^{-5}. Significant questions about tuning of the original selection of Bl-Lacs remain and an independent data set will shortly be analyzed to confirm or refute this apparent correlation.

If the correlation holds up, it will certainly be very interesting since only neutral particles can show a correlation within the intrinsic angular resolution of the detector and, given the ~100 Mpc distances to Bl Lacs, it is very unlikely that photons would survive.

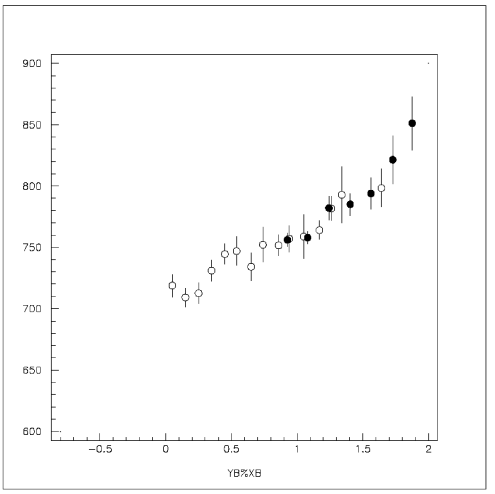

Fig. 12. Upadated elongation rate. Solid circles – "golden events"; open circles – original HiRes stereo data

10. Neutrino flux search

Many of the hypothetical sources of cosmic rays that have been proposed could also be sources of ultra-high energy neutrinos [17]. A "bottom line" source of neutrinos will result from the GZK mechanism itself. While the predictions of the GZK neutrino flux depend on the evolution of the sources of ultra-high energy cosmic rays themselves, there is no question that this represents a certain, albeit weak, flux. Previous air-fluorescence experiments have set limits on the electron neutrino flux [18]. A conference paper in this proceedings by Kai Martens describes a search for the tau-neutrino flux using the detailed topography of the region around the HiRes detectors as a target mass. Since the existence of neutrino oscillations implies equal fluxes of electron, muon and tau neutrinos, this channel turns out to be quite sensitive and is beginning to impinge on the more optimistic GZK flux predictions.

11. Conclusion

The HiRes experiment has completed data taking as of March, 2006. HiRes I has currently the world's largest air-fluorescence data set on cosmic rays with energies > 3 EeV and has been accumulating data for ~ 9 years. HiRes II has been accumulating data for six years and has an extensive data set ranging down to .2 EeV. The HiRes stereo data set is now in the final analysis phase. The current stereo spectrum strongly confirms the presence of the ankle and GZK cutoff features seen in the monocular data. Stereo data indicates a light composition from above 1 EeV all the way to the GZK cutoff energy region. Previous suggestions of a correlation between cosmic ray arrival directions and a catalogue of Bl-Lac objects have been weakly confirmed, but additional analysis of independent data is needed to establish an objective probability for this correlation.

With the funding of the Telescope Array Experiment (see papers in this proceedings by S. Yoshida) in Millard County, Utah, the equipment used in the HiRes experiment will acquire a new life as it will be refurbished and moved to this location. It will be used to provide one of the three air-fluorescence sites for the main hybrid array and will also be used to extend the low energy threshold of the experiment to 300 PeV.

REFERENCES

1. J.N Matthews, S.B. Thomas et al., Proceedings of "the 28th International Cosmic Ray Conference", Tskuba, Japan, 911 (2003).

2. R. Abbasi et al., Astropart. Phys. 25 (2006) 93; R. Abbasi et al., .Astropart. Phys., to be published (2006), astro-ph/05124233.

3. Kakimoto et al., Nucl. Inst. Meth. A372, (1996) 527; M.Nagano et al., Astropart. Phys. 22 (2004) 235.

4. J. Belz et al., submitted to Astropart. Phys., (2006); astro-ph 0506741.

5. J. Belz et al., submitted to Astropart. Phys., (2006); astro-ph/0510375.

6. R. U. Abbasi et al., Phys. Rev. Lett, 92 (2004) 151101.

7. R. U. Abbasi et al., Phys. Lett. B 19 (2005) 271.

8. K. Greisen, Phys. Rev. Lett., 16 (1968) 48; G. T. Zatsepin and V. A. Kuzmin, Pis'ma Zh. Eksp. Teor. Fiz. 4 (1966) 114.

9. G. L. Cassiday et al., Ap. J. 356 (1990) 669; Phys. Rev. D 47 (1993) 1919.

9.

10. R. Engel, Proceedings of "Physics at the End of the Galactic Cosmic Ray Spectrum" Aspen (2005).; R. Engel, Nucl. Phys. B (Proc. Suppl.) 122 (2003).

11. R. U. Abbasi et al, Ap. J. 622 (2005) 910.

12. T. Abu-Zayyad, Ap. J. 557 (2001) 686

13. R.U. Abbasi et al., Astropart. Phys. 22 (2004) 139; R. U. Abbasi et al., Ap. J. 610(2004) L73.

14. D.S. Gorbunov et al., JETP Lett. (2004) 145.

15. P.G. Tinyakov, I.I.Tkachev JETP Lett. 74 (2002) 445; Astropart. Phys. 18 (2002) 165.

16. R. U. Abbasi et al., Ap. J. 636 (2006) 680.

17. APS Neutrino Study, Report of the Neutrino Astrophysics and Cosmology Working Group (2004); D. Semikoz, Proceedings of ' the 28th International Cosmic Ray Conference", Tskuba, Japan,1439 (2003).

18. R. Baltrusaitis et al., Phys. Rev D 31 (1985)) 2129; Ap.J. 281 (1984) L9.